BRAIN CONNECTIVITY
Volume 7, Number 2, 2017

DOI: 10.1089/brain.2016.0457

Topological Organization of Whole-Brain White Matter in HIV Infection

Laurie M. Baker,[1,*] Sarah A. Cooley,[2,*] Ryan P. Cabeen,[3] David H. Laidlaw,[4] John A. Joska,[5] Jacqueline Hoare,[5] Dan J. Stein,[5,6] Jodi M. Heaps-Woodruff,[7] Lauren E. Salminen,[3] and Robert H. Paul[1,7]

Abstract

Infection with human immunodeficiency virus (HIV) is associated with neuroimaging alterations. However, little is known about the topological organization of whole-brain networks and the corresponding association with cognition. As such, we examined structural whole-brain white matter connectivity patterns and cognitive performance in 29 HIV+ young adults (mean age = 25.9) with limited or no HIV treatment history. HIV+ participants and demographically similar HIV− controls ($n = 16$) residing in South Africa underwent magnetic resonance imaging (MRI) and neuropsychological testing. Structural network models were constructed using diffusion MRI-based multifiber tractography and T_1-weighted MRI-based regional gray matter segmentation. Global network measures included whole-brain structural integration, connection strength, and structural segregation. Cognition was measured using a neuropsychological global deficit score (GDS) as well as individual cognitive domains. Results revealed that HIV+ participants exhibited significant disruptions to whole-brain networks, characterized by weaker structural integration (characteristic path length and efficiency), connection strength, and structural segregation (clustering coefficient) than HIV− controls ($p < 0.05$). GDSs and performance on learning/recall tasks were negatively correlated with the clustering coefficient ($p < 0.05$) in HIV+ participants. Results from this study indicate disruption to brain network integrity in treatment-limited HIV+ young adults with corresponding abnormalities in cognitive performance.

Keywords: cognition; HIV; network analysis; whole-brain connectivity

Introduction

The human immunodeficiency virus (HIV) crosses the blood–brain barrier shortly after seroconversion (~8 days) and before marked immune suppression and overt cognitive dysfunction (Valcour et al., 2012). Despite the efficacy of combination antiretroviral therapy (cART) in reducing viral load, current treatments do not appear to prevent or reverse existing brain damage (Ances et al., 2012; Harezlak et al., 2011; Heaton et al., 2011). Importantly, research shows axonal disruption and synaptic injury after HIV infection (Avdoshina et al., 2013; Ellis et al., 2007; Everall et al., 1999, 2009; Masliah et al., 1997). Although specific brain regions appear uniquely vulnerable, HIV-mediated neuronal damage is present throughout the brain (Ellis et al., 2007; Ragin et al., 2004) and corresponds to neuropsychological dysfunction (Masliah et al., 1997).

Diffusion tensor imaging (DTI) provides a robust method for identifying disruptions to the structural connections throughout the brain. Multiple studies utilizing DTI reveal abnormalities in brain white matter capable of disrupting connectivity across brain regions in HIV+ individuals (Filippi et al., 2001; Gongvatana et al., 2009; Hoare et al., 2011; Ragin et al., 2004; Thurnher et al., 2005). Furthermore, using complex network analysis, structural changes in white matter connections can be effectively modeled by combining diffusion magnetic resonance imaging (MRI)-based tractography and

[1]Department of Psychology, University of Missouri–Saint Louis, Saint Louis, Missouri.
[2]Department of Neurology, School of Medicine, Washington University in Saint Louis, Saint Louis, Missouri.
[3]Keck School of Medicine, University of Southern California, Los Angeles, California.
[4]Computer Science Department, Brown University, Providence, Rhode Island.
[5]Department of Psychiatry and Mental Health, University of Cape Town, Cape Town, South Africa.
[6]MRC Unit on Anxiety & Stress Disorders, Cape Town, South Africa.
[7]Missouri Institute of Mental Health, St. Louis, Missouri.
*Co-first authors.

T_1-weighted MRI-based regional gray matter segmentation. This network-based approach is highly sensitive to alterations in brain integrity across multiple disease pathologies including schizophrenia, Alzheimer's disease, and major depressive disorder (Bassett, 2010; Bassett et al., 2008; Bullmore and Sporns, 2009; He et al., 2008; Lo et al., 2010; Yu et al., 2011; Zhang et al., 2011).

Complex network analysis has been recently applied to investigate signatures of HIV neuropathogenesis (Jahanshad et al., 2012). In this study, significant disruptions to brain connectivity were identified in older HIV+ adults on cART. However, the relationship between the topological organization of white matter and cognitive function in HIV remains unclear. Furthermore, no studies have examined connectivity metrics (e.g., structural segregation, structural integration, and connection strength) in younger HIV+ individuals. It is necessary to fill this gap in the literature to determine the functional relevance of white matter connectivity in HIV+ individuals, independent of advanced age.

We used diffusion MRI-based tractography and graph-theoretic approaches to investigate the topological organization of white matter in 29 HIV+ young adults and 16 HIV− demographically similar controls utilizing fiber-bundle length (FBL)-defined whole-brain connectivity metrics (structural segregation, structural integration, and connection strength). These metrics provide insight into communication between regions of the brain. We also examined the relationship between whole-brain topological organization and cognitive performance using a global deficit score (GDS) and individual cognitive domain deficit scores (learning/recall, psychomotor/processing speed, executive function, fine motor skills and dexterity, and visuospatial skills). We hypothesized that whole-brain topological organization would be diminished in HIV+ individuals compared with HIV− controls, and the degree of abnormalities in the three connectivity metrics would significantly correlate with poorer cognitive performance in young HIV+ individuals.

Methods

Participants

HIV+ participants were recruited from primary care HIV clinics in Cape Town, South Africa. Patients who were in the pretreatment counseling phase were identified from clinic records. Interested participants completed a comprehensive consent process followed by a detailed medical and demographic history. All participants were either treatment naive at enrollment (83%) or had initiated cART within 3 months of enrollment (17%). All but five participants began treatment within 1 month of enrollment. HIV− participants were recruited from regional Voluntary Counseling and Testing Clinics in Cape Town, South Africa. Table 1 provides demographic information for the 29 HIV+ and 16 HIV− participants.

Inclusion criteria for HIV+ participants included (1) age between the years of 18 and 45; (2) Xhosa as the primary language; (3) HIV serostatus documented by ELISA and confirmed by Western blot, plasma HIV RNA, or a second antibody test for the HIV+ group; and (4) at least 7 years of formal education (all but one participant reported at least 10 years of education). Exclusion criteria for all participants included (1) any major psychiatric condition that could significantly affect cognitive status (e.g., schizophrenia or bipolar disorder); (2) confounding neurological disorders including multiple sclerosis and other central nervous system (CNS) conditions; (3) head injury with loss of consciousness greater than 30 min; (4) clinical evidence of opportunistic CNS infections (toxoplasmosis, progressive multifocal leukoencephalopathy, and neoplasms); and (5) current substance use disorder determined by the Mini-International Neuropsychiatric Interview Plus (MINIPlus) (Sheehan et al., 1998). All participants provided signed informed consent. Study procedures were approved by local university IRB committees.

HIV viral load and CD4 T cell counts

EDTA blood samples were collected at the time of study visit and plasma and cell aliquots were stored at −70°C. RNA was isolated from patient samples using the Abbott RealTime HIV-1 amplification reagent kit, according to the manufacturer's instructions. Viral load was determined using the Abbott m2000sp and the Abbott m2000rt analyzers (Abbott laboratories, Abbott Park, IL). All HIV+ participants had a detectable viral load (range 183–1,759,510 copies/mL). Analyses of cells from fresh blood samples were completed on the FACSCalibur flow cytometer in conjunction

Table 1. Subject Characteristics

	HIV+ (n = 29)	*HIV− (n = 16)*	p
Mean age ± SD (range)	25.89 ± 2.12 (22–29)	24.69 ± 4.53 (20–32)	0.55
Mean education ± SD (range)	10.76 ± 0.69 (10–12)	10.94 ± 1.29 (7–12)	0.31
Sex (% male)	17%	31%	0.46
Mean recent CD4 (cells/mm^3) ± SD (range)	249.79 ± 164.23 (35–799)		
Mean plasma VL (copies/mL)[a] ± SD (range)	4.21 ± 1.06 (2.26–6.25)		
Mean months of infection ± SD (range)	9.33 ± 19.56 (0–97)		
% prescribed antiretroviral therapy	17%		
Mean intracranial volume (cm^3) ± SD (range)	1307.15 ± 246.69 (1027.86–1728.54)	1345.50 ± 211.64 (961.03–2033.13)	0.60
Mean global deficit score ± SD (range)	0.34 ± 0.32 (0–1)	0.18 ± 0.22 (0–0.82)	0.06

[a]Viral load $\log_{10}$ transformed.
HIV, human immunodeficiency virus.

with the MultiSET V1.1.2 software (BD Biosciences, San Jose, CA) for CD4 T cell counts.

Neuroimaging acquisition

Neuroimaging was acquired on a 3T Siemens Allegra scanner (Siemens AG, Erlangen, Germany), with a four-channel phased-array head coil. Thirty unique diffusion gradient directions at $b = 1000\,sec/mm^2$ were repeated to give a total of 60 diffusion weighted volumes using a customized single-shot multislice echo-planar tensor-encoded imaging sequence. Six baseline images were acquired and interleaved in the diffusion-weighted scans to improve motion correction. Seventy contiguous slices were obtained per contrast with a 128×128 matrix and field of view of $218 \times 218\,mm$ (isotropic $1.7 \times 1.7 \times 1.7\,mm^3$ voxels); time of repetition (TR): 10 sec, echo time (TE): 103 ms using a full-Fourier transform. We also acquired a T_1-weighted three-dimensional magnetization-prepared rapid acquisition gradient echo sequence (TR = 2400 ms, TE = 2.38 ms, inversion time [TI] = 1000 ms flip angle = 8°, 162 slices, and voxel size = $1 \times 1 \times 1$ mm^3 for volumetric analyses).

Neuroimaging analysis

The T_1-weighted MR images were processed with Freesurfer version 5.1.0 (Fischl, 2012) to obtain a high-resolution gray matter parcellation. The diffusion-weighted MR images were processed with a pipeline including FSL 5.0 (Jenkinson et al., 2012) and custom software, described as follows. First, FSL eddy current was used to correct for motion and eddy currents by registering each diffusion-weighted volume to the first baseline with an affine transformation. The gradient-encoding vectors were also rotated to account for the spatial transformation of each volume (Leemans and Jones, 2009). Then, FSL BET was run for brain extraction, and XFIBRES was run to obtain ball-and-sticks diffusion models in each voxel (Behrens et al., 2007). Model fitting was performed with two stick compartments to improve tractography in areas with complex anatomy, such as crossing fibers. Whole-brain deterministic streamline tractography was performed to obtain geometric models of white matter pathways.

Tractography was executed utilizing an extension of the standard streamline approach to use multiple fibers per voxel with the following parameters: four seeds per voxel, an angle threshold of 50°, a minimum length of 10 mm, and a minimum volume fraction of 0.1. During tracking, a kernel regression estimation framework (Cabeen et al., 2016) was used for smooth interpolation of the multifiber ball-and-sticks models with a Gaussian kernel using a spatial bandwidth of 1.5 mm and window of 1 mm voxels of $7 \times 7 \times 7$. Then a subject-specific structural network model was constructed from the combination of diffusion MR tractography and T_1-weighted MRI gray matter labels from the Desikan–Killiany atlas (Desikan et al., 2006) and subcortical segmentations obtained from Freesurfer. For each pair of regions, a structural connection was defined by first selecting fibers with end-points in pairs of gray matter areas and then computing the average FBL of the selected fibers to represent connection strength (Correia et al., 2008). To avoid resampling artifacts, the tractography was performed in native space and then the curve data were transformed to T_1-space to test for intersection with gray matter regions. This step registered the T_1-weighted MRI to the average baseline diffusion scan using FSL FLIRT with the mutual information criteria and an affine transformation. The resulting weighted undirected connectivity matrix was analyzed with the Brain Connectivity Toolbox (http://https://sites.google.com/site/bctnet/) to obtain global network measures of connection strength, structural segregation (clustering coefficient), and structural integration (characteristic path length and global efficiency) (Fig. 1; Rubinov and Sporns, 2010).

Neuropsychological evaluation

The neuropsychological battery included tests of the following domains: Learning/recall—(1) Hopkins Verbal Learning Test-Revised (HVLT-R; Brandt and Benedict, 2001) and (2) Brief Visuospatial Memory Test-Revised

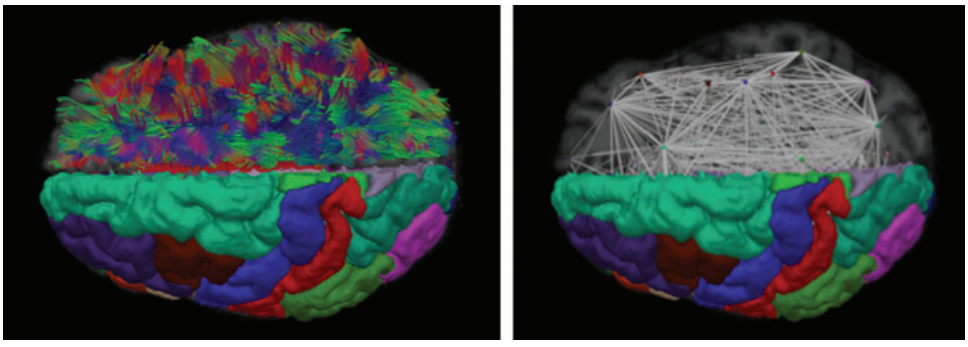

FIG. 1. Structural network analysis visualizations. Left: A visualization of imaging-based reconstructions of anatomy, showing diffusion magnetic resonance imaging (MRI)-based tractography and T1-weighted MRI-based gray matter segmentations. The left hemisphere shows Desikan–Killiany regions-of-interest and the right hemisphere shows streamline tractography curves used to define connectivity between regions. Right: A visualization of a structural network model derived from neuroimaging data. The left hemisphere shows Desikan–Killiany regions-of-interest and the right hemisphere shows a node-link diagram representing the topological organization of white matter. Nodes are placed at the centroid of each region and the links are derived from the average fiber bundle length between the pairs of regions with structural connections. Color images available online at www.liebertpub.com/brain

(BVMT-R; Benedict et al., 1996). Total correct on the immediate and delayed recall trials was defined as the dependent variables for the HVLT-R and BVMT-R. Psychomotor/processing speed—(1) Color Trails 1 (D'Elia and Satz, 1996), (2) Trail Making Test A (Reitan, 1955), and (3) Digit Symbol (Wechsler et al., 2008). Time to completion was the dependent variable for Color Trails 1 and Trail Making Test A. Total correct was the dependent variable for Digit Symbol. Executive function—(1) Color Trails 2 (D'Elia and Satz, 1996) and (2) Wisconsin Card Sorting Test (WCST; Heaton et al., 1993). Time to completion was the dependent variable for Color Trails 2, and total perseveration errors served as the dependent variable for the WCST. Visuospatial skills—Block Design from the WAIS-IV (Wechsler, 1997). Total correct was the dependent variable. Fine motor skills and dexterity—Grooved Pegboard Test (Kløve, 1963) nondominant hand. Time to completion was the dependent variable.

Determination of domain-specific and global neuropsychological function

For data reduction purposes, raw data from the neuropsychological test battery were converted to T scores using mean and standard deviations from a sample of 52 HIV− individuals recruited from South Africa. A deficit score (ranging from 0 to 5 with a score of 0 indicating normal range and greater scores indicating greater impairment) for each test was determined using the methods previously reported by Carey et al. (2004). This approach provides a more sensitive method for generating a summary neuropsychological score than averaging neuropsychological scores (Carey et al., 2004; Heaton et al., 2004). A GDS was then obtained for each participant, with higher scores indicative of greater impairment. A GDS provides a continuous measure of impairment with scores >0.5 providing high rates of specificity (0.89) and positive predictive value (0.83) in establishing HIV-associated impairment (Carey et al., 2004; Heaton et al., 2004).

Domain-specific deficit scores were calculated using methods similar to the calculation for the GDS. Specifically, standardized T scores for each neuropsychological test were converted to a deficit score between 0 and 5. The deficit scores were averaged to determine domain-specific deficit scores (i.e., learning/recall, psychomotor/processing speed, executive function, fine motor skills and dexterity, and visuospatial skills).

Statistical analysis

All statistical analyses were conducted utilizing SPSS, version 24. Differences in age, sex, and education between HIV+ and HIV− participants were examined using independent sample *t*-tests (age and education) and chi-squared analyses (sex) to determine potential covariates for the primary analyses. Differences in whole-brain topological organization between groups were examined using three separate analyses of covariance or multivariate analyses of covariance (ANCOVA/MANCOVA) models, depending on the number of metrics in each category. HIV serostatus served as the independent variable and individual measures of topological organization served as dependent variables in each analysis, with intracranial volume as a covariate. The measures of topological organization included structural segregation (clustering coefficient), structural integration (characteristic path length and global efficiency), and connection strength. Viral load was natural log transformed to achieve a normal distribution for correlation analyses. Pearson's correlations were used to determine whether individual measures of connectivity were significantly related to HIV clinical variables (CD4 T cell count and log-transformed viral load).

With respect to the distribution of GDS and domain-specific deficit scores, the standardized skewness coefficients and the standardized kurtosis coefficients revealed significant departures from normality in the entire sample and within the HIV+ group. Therefore, a nonparametric procedure, Spearman's rank order correlation (i.e., Spearman's rho), was performed to address all correlations that included the GDS or domain scores. These analyses were performed within the HIV+ sample as well as collapsed across the HIV+ and HIV− groups.

Results

Subject characteristics are listed in Table 1. There were no statistically significant differences in demographic factors (age, education, and sex) between HIV+ and HIV− participants. The ANCOVA/MANCOVA models revealed significantly weaker structural segregation in HIV+ participants, defined by a lower clustering coefficient ($F(1,42) = 11.20$, $p = 0.002$), Cohen's $d = 1.06$), as well as weaker structural integration defined by higher characteristic path length and lower global efficiency (Wilks' $\Lambda = 0.77$, $F(2,41) = 6.10$, $p = 0.005$, $d = 0.79$), with characteristic path length $F(1,42) = 12.23$, $p = 0.001$, $d = 1.12$) and global efficiency $F(1,41) = 12.33$, $p = 0.001$, $d = 1.12$) both significantly contributing to the model. Lastly, HIV+ participants showed weaker connection strength ($F(1,42) = 8.29$, $p = 0.006$, $d = 0.92$) (Table 2). Pearson's correlational analyses revealed that CD4 T cell count and viral load were not significantly associated with any individual measures of connectivity ($r < |0.30|$; $p > 0.05$).

Relationships between GDSs and connectivity metrics

Collapsed across HIV+ and HIV− participants, Spearman's rho revealed statistically significant correlations between GDSs with global characteristic path length ($r = 0.34$, $p = 0.027$) and mean connection strength ($r = -0.31$, $p = 0.046$). Trend level

Table 2. Differences in Network Connectivity Between HIV+ and HIV− Participants

	HIV+ (n = 29)	*HIV− (n = 16)*	p
Global clustering coefficient (mm)	53.18 (4.47)	57.67 (3.37)	0.002
Global characteristic path length (1/mm)	0.015 (0.0012)	0.013 (0.0009)	0.001
Global efficiency (mm)	77.86 (7.17)	85.62 (6.54)	0.001
Global connection strength (mm)	2939.75 (385.99)	3271.76 (312.58)	0.006

Values are represented in mean (SD).

relationships were also observed with global efficiency ($r=-0.30$, $p=0.057$) and clustering coefficient ($r=-0.30$, $p=0.055$). Together, these results indicate that poorer cognitive performance is associated with abnormal network indices. When examined specifically within the HIV+ sample, Spearman's rho showed statistically significant negative relationships between the GDS and the clustering coefficient ($r=-0.40$, $p=0.042$), and trend level negative associations with global efficiency ($r=-0.38$, $p=0.056$) and connection strength ($r=-0.37$, $p=0.062$). A trend level positive relationship was observed between the GDS and characteristic path length ($r=0.37$, $p=0.060$).

Relationships between domain-specific deficit scores and connectivity metrics

Collapsed across HIV+ and HIV− participants, poorer learning/recall was significantly associated with higher global characteristic path length ($r=0.36$, $p=0.010$), lower mean connection strength ($r=-0.37$, $p=0.012$), lower global efficiency ($r=-0.36$, $p=0.016$), and lower clustering coefficient ($r=-0.39$, $p=0.009$). No other significant relationships were observed between the brain connectivity metrics and psychomotor/processing speed, executive function, fine motor skills and dexterity, or visuospatial skills ($r<|0.30|$, $p>0.05$). When examined specifically within the HIV+ sample, learning/recall deficit scores were significantly negatively associated with the clustering coefficient ($r=-0.40$, $p=0.037$). Negative trend level relationships were observed between learning/recall deficit scores and mean connection strength ($r=-0.36$, $p=0.064$) and global efficiency ($r=-0.36$, $p=0.058$), whereas a trend level positive relationship was observed with global characteristic length ($r=0.36$, $p=0.052$). No significant relationships were observed between the connectivity metrics and psychomotor/processing speed, executive function, fine motor skills, and dexterity, or visuospatial skills ($r<|0.30|$, $p>0.05$) in the HIV+ sample.

Discussion

This study revealed topological disorganization of brain white matter in HIV, including abnormalities in structural segregation, structural integration, and connection strength. Furthermore, these abnormalities in network connectivity metrics were significantly associated with cognitive dysfunction both across the entire sample and specifically within the HIV+ group. These abnormalities were not significantly related to HIV clinical status (CD4 T cell count and viral load). Findings indicate that younger HIV+ participants with limited or no antiretroviral treatment history exhibit significantly altered measures of whole-brain connectivity relative to demographically similar HIV− controls. These data suggest that alterations in whole-brain network disruption are behaviorally relevant in the context of HIV.

Structural segregation refers to neural processing within interconnected regions of the brain, whereas structural integration refers to the potential to rapidly combine specialized information from distributed brain networks. The interplay of segregation and integration in brain networks generates information that is simultaneously diversified and synthesized, resulting in patterns of high complexity. Extensive research indicates that the dynamic patterns generated by these networks provide the basis for cognition and perception (Bressler and Kelso, 2001; Frackowiak, 2004; McIntosh, 1999; Varela et al., 2001). Underlying these global properties is a measure of connectivity between brain regions, which we examined with the average FBL of tractography curves. Overall lower structural segregation (clustering coefficient), structural organization (characteristic path length and global efficiency), and connection strength were observed, indicating that HIV is associated with abnormal whole-brain network connectivity.

Neuroimaging studies have revealed consistent disruptions to subcortical and cortical brain structures among individuals infected with HIV (Ances et al., 2012; Archibald et al., 2004; Becker et al., 2011; Berger and Arendt, 2000; Cohen et al., 2010; Heaps et al., 2012; Ragin et al., 2012; Stout et al., 1998). Specifically, reduced volumes have been observed within the thalamus, caudate, putamen, hippocampus, cortical white matter, and gray matter (Ances et al., 2012; Holt et al., 2012; Ortega et al., 2013; Paul et al., 2008, 2016; Thompson et al., 2005). Individuals with more advanced disease exhibit reduced cortical thickness in primary sensory and motor areas (Thompson et al., 2005), possibly reflecting distal effects of basal ganglia damage. Results from Jahanshad et al. (2012) revealed pronounced white matter network disruption in primary motor and sensory areas of the parietal and frontal lobes of older HIV individuals on stable treatment. Our study extends previous work by revealing global network disruption in younger HIV+ individuals with immune suppression and limited or no treatment history.

DTI abnormalities observed using scalar metrics in frontal, callosal, and deep white matter regions in HIV+ individuals have been associated with poor cognitive performance (Chang et al., 2008; Chen et al., 2009; Hoare et al., 2015; Jernigan et al., 1993; Müller-Oehring et al., 2010; Ortega et al., 2013; Pomara et al., 2001; reviewed in Hardy and Hinkin, 2002; Stout et al., 1998; Thurnher et al., 2005). Our results reveal a strong association between cognitive dysfunction and diffuse brain network disruption in HIV+ young adults. Collapsed across HIV+ and HIV− participants, we observed significant associations between both GDS and learning/recall with structural integration (characteristic path length) and connection strength, indicative of reduced information transfer across networks (Latora and Marchiori, 2001) and reduced FBL. Conversely, the most prominent relationships in the HIV+ group were observed between structural segregation (clustering coefficient) and both global neuropsychological impairment and learning/recall. This pattern of structural abnormalities provides evidence of cognitive impairment related to a measure of neural processing within densely interconnected networks.

Inflammation is hypothesized to be one of many important drivers of neuronal injury and loss in HIV. Inflammation occurs soon after viral entry into the CNS and is associated with the release of proinflammatory cytokines, chemokines, and neurotoxic viral proteins in response to HIV-infected macrophages and microglia (Anthony et al., 2005; Harezlak et al., 2011; Lentz et al., 2011; Sailasuta et al., 2012; Valcour et al., 2012; Vera et al., 2016). In turn, these activate uninfected macrophages and microglia to further release neurotoxic substances that lead to compromised synaptodendritic connections, damage to axonal and myelin integrity, and potentially neuronal death (Conant et al., 1998; Raja et al., 1997).

These injuries are distributed widely throughout the brain and correspond to white matter damage (Ellis et al., 2007) as well as cognitive impairment (Everall et al., 1999).

An advantage of our study is the tractography method employed to quantify structural connectivity. Typically, a major challenge of estimating whole-brain connectivity metrics is the presence of complex configurations of fiber bundle anatomy such as fiber crossings. The diffusion tensor model does not accurately represent voxels consisting of multiple fiber populations, which limits the anatomical validity of network models derived using single tensor models. More sophisticated techniques that represent multiple fibers, such as multicompartment and high angular resolution diffusion imaging, offer greater anatomical accuracy and improved sensitivity in detecting complex anatomical features related to white matter changes caused by disease (Tuch et al., 1999, 2002). We used the ball-and-sticks multicompartment model (Behrens et al., 2007) and a model-based estimation framework (Cabeen et al., 2016) to improve the accuracy of connectivity mapping. Importantly, although this approach is ideal for the single shell data, more sophisticated microstructure models that utilize multishell acquisitions may provide improved anatomical accuracy and sensitivity to detect white matter changes. Future studies may benefit by using neurite orientation dispersion and density imaging to characterize changes in neurite density and orientation dispersion (Zhang et al., 2012).

Several limitations are important to address. First, we did not have sufficient number of male HIV+ participants to examine sex differences in brain network topology. Previous research conducted in HIV− populations reveals sex differences in brain topology (Gong et al., 2009; Yan et al., 2011), emphasizing the importance of examining sex differences in future studies. In addition, future research is needed to determine whether treatment improves whole-brain connectivity abnormalities. Lastly, we excluded participants with substance use disorder because of evidence that structural connectivity is disrupted in substance users independent of HIV (Bava et al., 2009; Kim et al., 2014). Our approach ensured that the observed effects were not confounded by substance use. However, our results may not generalize to the population of HIV+ substance users. Despite these limitations, our findings provide strong evidence for functionally relevant disruptions to network organization in HIV.

Conclusions

This article extends the literature in three novel ways. First, our cohort comprised young HIV+ adults. Second, our sample was predominantly free of treatment confounds on brain connectivity. Lastly, the present study included measures of cognition that inform the functional relevance of the connectivity measures. Collectively, the results support a model of diffuse network changes in young HIV+ individuals with limited or no treatment history and corresponding cognitive dysfunction. The results provide further evidence of the utility of anatomical brain connectivity as a noninvasive biomarker of white matter disruption in HIV infection.

Acknowledgments

This study was supported by the National Institute of Mental Health (MH085604). Dr. Stein was supported by the Medical Research Council of South Africa.

Author Disclosure Statement

No competing financial interests exist.

References

Ances BM, Ortega M, Vaida F, Heaps J, Paul R. 2012. Independent effects of HIV, aging, and HAART on brain volumetric measures. J Acquir Immune Defic Syndr 59:469.

Anthony IC, Ramage SN, Carnie FW, Simmonds P, Bell JE. 2005. Influence of HAART on HIV-related CNS disease and neuroinflammation. J Neuropathol Exp Neurol 64:529–536.

Archibald SL, Masliah E, Fennema-Notestine C, Marcotte TD, Ellis RJ, McCutchan JA, Jernigan TL. 2004. Correlation of in vivo neuroimaging abnormalities with postmortem human immunodeficiency virus encephalitis and dendritic loss. Arch Neurol 61:369–376.

Avdoshina V, Bachis A, Mocchetti I. 2013. Synaptic dysfunction in human immunodeficiency virus type-1-positive subjects: inflammation or impaired neuronal plasticity? J Intern Med 273:454–465.

Bassett DS. 2010. Clinical applications of complex network analysis. In: Sporns O (ed.) *Short Course III-Analysis and Function of Large-Scale Brain Networks*. Washington, DC: Society for Neuroscience; pp. 55–63.

Bassett DS, Bullmore E, Verchinski BA, Mattay VS, Weinberger DR, Meyer-Lindenberg A. 2008. Hierarchical organization of human cortical networks in health and schizophrenia. J Neurosci 28:9239–9248.

Bava S, Frank LR, McQueeny T, Schweinsburg BC, Schweinsburg AD, Tapert SF. 2009. Altered white matter microstructure in adolescent substance users. Psychiatry Res 173: 228–237.

Becker JT, Sanders J, Madsen SK, Ragin A, Kingsley L, Maruca V, Sacktor N. 2011. Subcortical brain atrophy persists even in HAART-regulated HIV disease. Brain Imaging Behav 5:77–85.

Behrens TEJ, Berg HJ, Jbabdi S, Rushworth MFS, Woolrich MW. 2007. Probabilistic diffusion tractography with multiple fibre orientations: what can we gain?. Neuroimage 34:144–155.

Benedict RH, Schretlen D, Groninger L, Dobraski M, Shpritz B. 1996. Revision of the brief visuospatial memory test: studies of normal performance, reliability, and validity. Psychol Assess 8:145.

Berger JR, Arendt G. 2000. HIV dementia: the role of the basal ganglia and dopaminergic systems. J Psychopharmacol 14:214–221.

Brandt J, Benedict RH. 2001. *Hopkins Verbal Learning Test—Revised: Professional Manual*. Lutz, FL: Psychological Assessment Resources.

Bressler SL, Kelso JS. 2001. Cortical coordination dynamics and cognition. Trends Cogn Sci 5:26–36.

Bullmore E, Sporns O. 2009. Complex brain networks: graph theoretical analysis of structural and functional systems. Nat Rev Neurosci 10:186–198.

Cabeen RP, Bastin ME, Laidlaw DH. 2016. Kernel regression estimation of fiber orientation mixtures in diffusion MRI. Neuroimage 127:158–172.

Carey CL, Woods SP, Gonzalez R, Conover E, Marcotte TD, Grant I, Heaton RK. 2004. Predictive validity of global deficit scores in detecting neuropsychological impairment in HIV infection. J Clin Exp Neuropsychol 26:307–319.

Chang L, Wong V, Nakama H, Watters M, Ramones D, Miller EN, Ernst T. 2008. Greater than age-related changes in

brain diffusion of HIV patients after 1 year. J Neuroimmune Pharmacol 3:265–274.

Chen Y, An H, Zhu H, Stone T, Smith JK, Hall C, Lin W. 2009. White matter abnormalities revealed by diffusion tensor imaging in non-demented and demented HIV+ patients. Neuroimage 47:1154–1162.

Cohen RA, Harezlak J, Schifitto G, Hana G, Clark U, Gongvatana A, Brown M. 2010. Effects of nadir CD4 count and duration of human immunodeficiency virus infection on brain volumes in the highly active antiretroviral therapy era. J Neurovirol 16:25–32.

Conant K, Garzino-Demo A, Nath A, et al. 1998. Induction of monocyte chemoattractant protein-1 in HIV-1 Tat-stimulated astrocytes and elevation in AIDS dementia. Proc Natl Acad Sci U S A 95:3117–3121.

Correia S, Lee SY, Voorn T, Tate DF, Paul RH, Zhang S, Laidlaw DH. 2008. Quantitative tractography metrics of white matter integrity in diffusion-tensor MRI. Neuroimage 42:568–581.

D'Elia L, Satz P. 1996. *Color Trails Test*. Odessa, FL: Psychological Assessment Resources.

Desikan RS, Ségonne F, Fischl B, Quinn BT, Dickerson BC, Blacker D, Killiany RJ. 2006. An automated labeling system for subdividing the human cerebral cortex on MRI scans into gyral based regions of interest. Neuroimage 31:968–980.

Ellis R, Langford D, Masliah E. 2007. HIV and antiretroviral therapy in the brain: neuronal injury and repair. Nat Rev Neurosci 8:33–44.

Everall I, Vaida F, Khanlou N, Lazzaretto D, Achim C, Letendre S, Morgello S. 2009. Cliniconeuropathologic correlates of human immunodeficiency virus in the era of antiretroviral therapy. J Neurovirol 15:360–370.

Everall IP, Heaton RK, Marcotte TD, Ellis RJ, McCutchan JA, Atkinson JH; HRNC Group. 1999. Cortical synaptic density is reduced in mild to moderate human immunodeficiency virus neurocognitive disorder. Brain Pathol 9: 209–217.

Filippi CG, Uluğ AM, Ryan E, Ferrando SJ, van Gorp W. 2001. Diffusion tensor imaging of patients with HIV and normal-appearing white matter on MR images of the brain. AJNR Am J Neuroradiol 22:277–283.

Fischl B. 2012. FreeSurfer. Neuroimage 62:774–781.

Frackowiak RS. 2004. *Human Brain Function*. San Diego: Academic Press.

Gong G, He Y, Concha L, Lebel C, Gross DW, Evans AC, Beaulieu C. 2009. Mapping anatomical connectivity patterns of human cerebral cortex using in vivo diffusion tensor imaging tractography. Cereb Cortex 19:524–536.

Gongvatana A, Schweinsburg BC, Taylor MJ, Theilmann RJ, Letendre SL, Alhassoon OM, Frank LR. 2009. White matter tract injury and cognitive impairment in human immunodeficiency virus-infected individuals. J Neurovirol 15:187–195.

Hardy DJ, Hinkin CH. 2002. Reaction time performance in adults with HIV/AIDS. J Clin Exp Neuropsychol 24:912–929.

Harezlak J, Buchthal S, Taylor M, Schifitto G, Zhong J, Daar ES, Cohen R. 2011. Persistence of HIV-associated cognitive impairment, inflammation and neuronal injury in era of highly active antiretroviral treatment. AIDS 25:625.

He Y, Chen Z, Evans A. 2008. Structural insights into aberrant topological patterns of large-scale cortical networks in Alzheimer's disease. J Neurosci 28:4756–4766.

Heaps JM, Joska J, Hoare J, Ortega M, Agrawal A, Seedat S, Paul R. 2012. Neuroimaging markers of human immunodeficiency virus infection in South Africa. J Neurovirol 18:151–156.

Heaton RK, Chelune GJ, Talley JL, Kay GG, Curtiss G. 1993. *Wisconsin Card Sorting Test: Manual*. Odessa, FL: Psychological Assessment Resources.

Heaton RK, Franklin DR, Ellis RJ, McCutchan JA, Letendre SL, LeBlanc S, Collier AC. 2011. HIV-associated neurocognitive disorders before and during the era of combination antiretroviral therapy: differences in rates, nature, and predictors. J Neurovirol 17:3–16.

Heaton RK, Marcotte TD, Mindt MR, Sadek J, Moore DJ, Bentley H, Grant I. 2004. The impact of HIV-associated neuropsychological impairment on everyday functioning. J Int Neuropsychol Soc 10:317–331.

Hoare J, Fouche JP, Phillips N, Joska JA, Paul R, Donald KA, Stein DJ. 2015. White matter micro-structural changes in ART-naive and ART-treated children and adolescents infected with HIV in South Africa. AIDS 29:1793–1801.

Hoare J, Fouche JP, Spottiswoode B, Sorsdahl K, Combrinck M, Stein DJ, Joska JA. 2011. White-matter damage in clade C HIV-positive subjects: a diffusion tensor imaging study. J Neuropsychiatry Clin Neurosci 23:308–315.

Holt JL, Kraft-Terry SD, Chang L. 2012. Neuroimaging studies of the aging HIV-1-infected brain. J Neurovirol 18:291–302.

Jahanshad N, Valcour VG, Nir TM, Kohannim O, Busovaca E, Nicolas K, Thompson PM. 2012. Disrupted brain networks in the aging HIV+ population. Brain Connect 2:335–344.

Jenkinson M, Beckmann CF, Behrens TE, Woolrich MW, Smith SM. 2012. FSL. Neuroimage 62:782–790.

Jernigan TL, Archibald S, Hesselink JR, Atkinson JH, Velin RA, McCutchan JA, Grant I. 1993. Magnetic resonance imaging morphometric analysis of cerebral volume loss in human immunodeficiency virus infection. Arch Neurol 50: 250–255.

Kim J, Parker D, Whyte J, Hart T, Pluta J, Ingalhalikar M, Verma R. 2014. Disrupted structural connectome is associated with both psychometric and real-world neuropsychological impairment in diffuse traumatic brain injury. J Int Neuropsychol Soc 20:887–896.

Kløve H. 1963. *Grooved Pegboard*. Lafayette, IN: Lafayette Instruments.

Latora V, Marchiori M. 2001. Efficient behavior of small-world networks. Phys Rev Lett 87:198701.

Leemans A, Jones DK. 2009. The B-matrix must be rotated when correcting for subject motion in DTI data. Magn Reson Med 61:1336–1349.

Lentz MR, Kim WK, Kim H, Soulas C, Lee V, Venna N, Gonzalez RG. 2011. Alterations in brain metabolism during the first year of HIV infection. J Neurovirol 17:220–229.

Lo CY, Wang PN, Chou KH, Wang J, He Y, Lin CP. 2010. Diffusion tensor tractography reveals abnormal topological organization in structural cortical networks in Alzheimer's disease. J Neurosci 30:16876–16885.

Masliah E, Ellis RJ, Mallory M, Heaton RK, Marcotte TD, Nelson JA, McCutchan JA. 1997. Dendritic injury is a pathological substrate for human immunodeficiency virus—related cognitive disorders. Ann Neurol 42:963–972.

McIntosh AR. 1999. Mapping cognition to the brain through neural interactions. Memory 7:523–548.

Müller-Oehring EM, Schulte T, Rosenbloom MJ, Pfefferbaum A, Sullivan EV. 2010. Callosal degradation in HIV-1 infection predicts hierarchical perception: a DTI study. Neuropsychologia 48:1133–1143.

Ortega M, Heaps JM, Joska J, Vaida F, Seedat S, Stein DJ, Ances BM. 2013. HIV clades B and C are associated with reduced brain volumetrics. J Neurovirol 19:479–487.

Paul RH, Ernst T, Brickman AM, Yiannoutsos CT, Tate DF, Cohen RA, Navia BA. 2008. Relative sensitivity of magnetic resonance spectroscopy and quantitative magnetic resonance imaging to cognitive function among nondemented individuals infected with HIV. J Int Neuropsychol Soc 14:725–733.

Paul RH, Phillips S, Hoare J, Laidlaw DH, Cabeen R, Olbricht GR, Salminen LE. 2016. Neuroimaging abnormalities in clade C HIV are independent of Tat genetic diversity. J Neurovirol 1–10.

Pomara N, Crandall DT, Choi SJ, Johnson G, Lim KO. 2001. White matter abnormalities in HIV-1 infection: a diffusion tensor imaging study. Psychiatry Res 106:15–24.

Ragin AB, Du H, Ochs R, Wu Y, Sammet CL, Shoukry A, Epstein LG. 2012. Structural brain alterations can be detected early in HIV infection. Neurology 79:2328–2334.

Ragin AB, Storey P, Cohen BA, Epstein LG, Edelman RR. 2004. Whole brain diffusion tensor imaging in HIV-associated cognitive impairment. AJNR Am J Neuroradiol 25:195–200.

Raja F, Sherriff FE, Morris CS, et al. 1997. Cerebral white matter damage in HIV infection demonstrated using beta-amyloid precursor protein immunore-activity. Acta Neuropathol (Berl) 93:184–189.

Reitan RM. 1955. The relationship of the trail making test to organic brain damage. J Consult Psychol 19:393–394.

Rubinov M, Sporns O. 2010. Complex network measures of brain connectivity: uses and interpretations. Neuroimage 52: 1059–1069.

Sailasuta N, Ross W, Ananworanich J, Chalermchai T, DeGruttola V, Lerdlum S, Spudich S. 2012. Change in brain magnetic resonance spectroscopy after treatment during acute HIV infection. PLoS One 7:e49272.

Sheehan DV, Lecrubier Y, Sheehan KH, Amorim P, Janavs J, Weiller E, Dunbar GC. 1998. The Mini-International Neuropsychiatric Interview (MINI): the development and validation of a structured diagnostic psychiatric interview for DSM-IV and ICD-10. J Clin Psychiatry 59 Suppl 20:22–33;quiz 34–57.

Stout JC, Ellis RJ, Jernigan TL, Archibald SL, Abramson I, Wolfson T, Grant I. 1998. Progressive cerebral volume loss in human immunodeficiency virus infection: a longitudinal volumetric magnetic resonance imaging study. Arch Neurol 55:161–168.

Thompson PM, Dutton RA, Hayashi KM, Toga AW, Lopez OL, Aizenstein HJ, Becker JT. 2005. Thinning of the cerebral cortex visualized in HIV/AIDS reflects CD4+ T lymphocyte decline. Proc Natl Acad Sci U S A 102:15647–15652.

Thurnher MM, Castillo M, Stadler A, Rieger A, Schmid B, Sundgren PC. 2005. Diffusion-tensor MR imaging of the brain in human immunodeficiency virus-positive patients. AJNR Am J Neuroradiol 26:2275–2281.

Tuch DS, Reese TG, Wiegell MR, Makris N, Belliveau JW, Wedeen VJ. 2002. High angular resolution diffusion imaging reveals intravoxel white matter fiber heterogeneity. Magn Reson Med 48:577–582.

Tuch DS, Weisskoff RM, Belliveau JW, Wedeen VJ. 1999. High angular resolution diffusion imaging of the human brain. In: Proceedings of the 7th Annual Meeting of ISMRM, Philadelphia, PA (Vol. 321).

Valcour V, Chalermchai T, Sailasuta N, Marovich M, Lerdlum S, Suttichom D, van Griensven F. 2012. Central nervous system viral invasion and inflammation during acute HIV infection. J Infect Dis 206:275–282.

Varela F, Lachaux JP, Rodriguez E, Martinerie J. 2001. The brainweb: phase synchronization and large-scale integration. Nat Rev Neurosci 2:229–239.

Vera JH, Guo Q, Cole JH, Boasso A, Greathead L, Kelleher P, Matthews PM. 2016. Neuroinflammation in treated HIV-positive individuals A TSPO PET study. Neurology 86: 1425–1432.

Wechsler D, III. *WAIS-III Administration and Scoring Manual*. San Antonio, TX: The Psychological Corporation, 1997.

Wechsler D, Coalson DL, Raiford SE. 2008. *WAIS-IV: Wechsler Adult Intelligence Scale*. San Antonio, TX: Pearson.

Yan C, Gong G, Wang J, Wang D, Liu D, Zhu C, He Y. 2011. Sex-and brain size-related small-world structural cortical networks in young adults: a DTI tractography study. Cereb Cortex 21:449–458.

Yu Q, Sui J, Rachakonda S, He H, Pearlson G, Calhoun VD. 2011. Altered small-world brain networks in temporal lobe in patients with schizophrenia performing an auditory oddball task. Front Syst Neurosci 5:7.

Zhang H, Schneider T, Wheeler-Kingshott CA, Alexander DC. 2012. NODDI: practical in vivo neurite orientation dispersion and density imaging of the human brain. Neuroimage 61: 1000–1016.

Zhang J, Wang J, Wu Q, Kuang W, Huang X, He Y, Gong Q. 2011. Disrupted brain connectivity networks in drug-naive, first-episode major depressive disorder. Biol Psychiatry 70:334–342.

Address correspondence to:
Laurie M. Baker
Department of Psychology
University of Missouri–Saint Louis
One University Boulevard
Stadler Hall 327
Saint Louis, MO 63121

E-mail: lauriebaker@umsl.edu